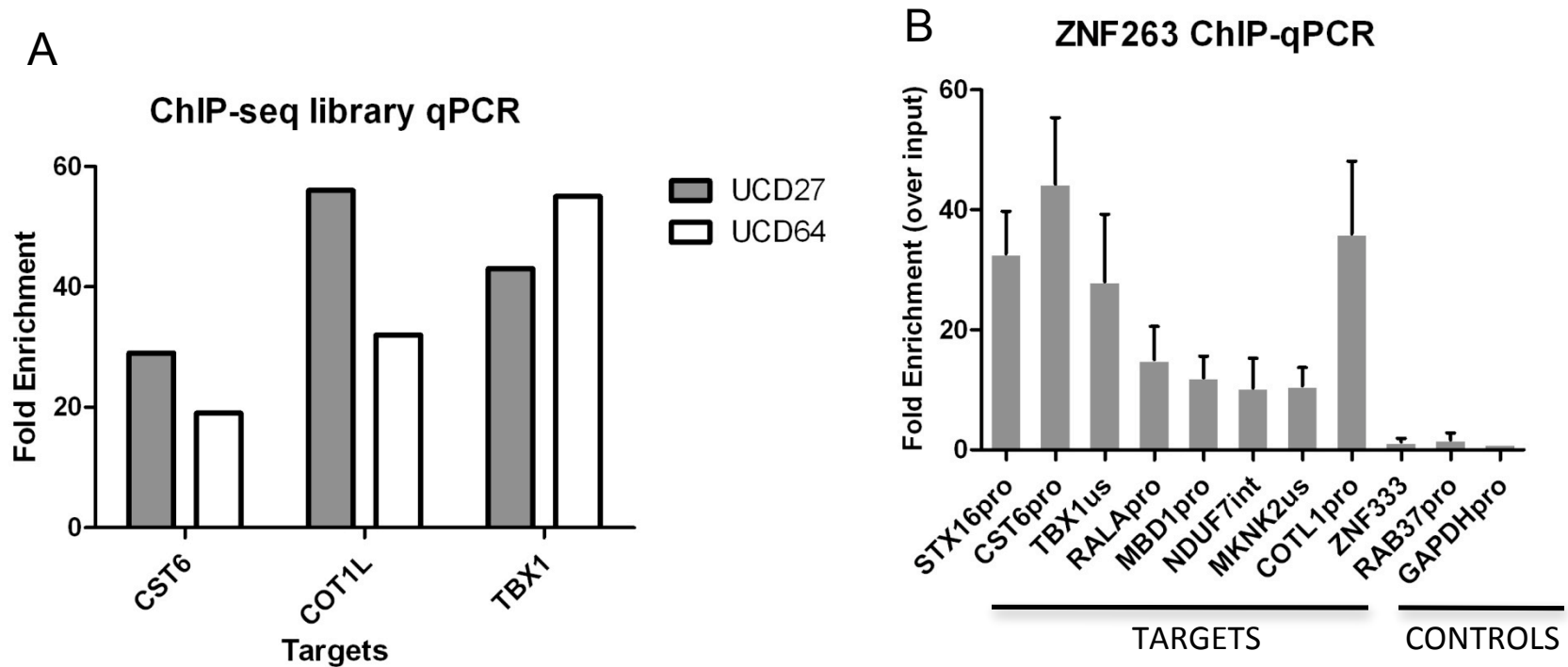
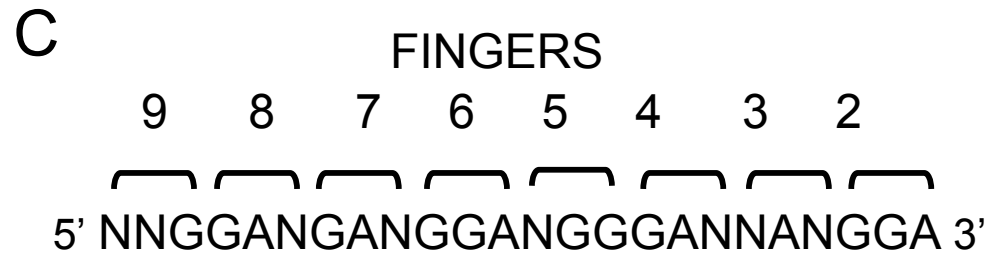
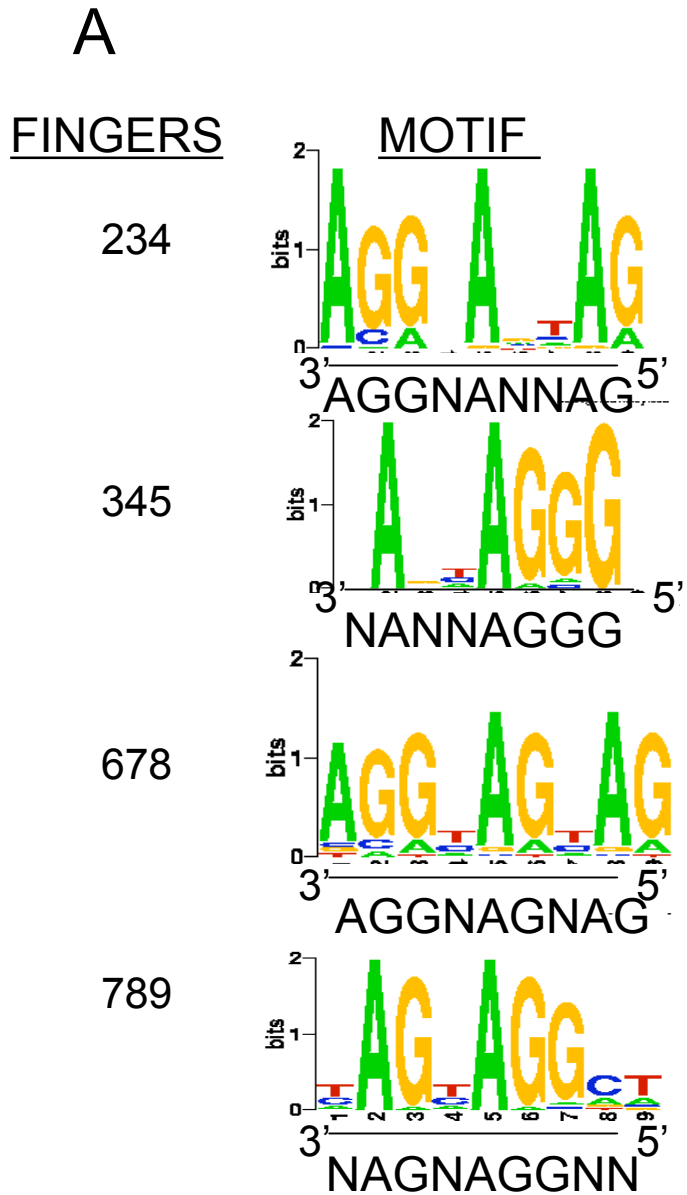


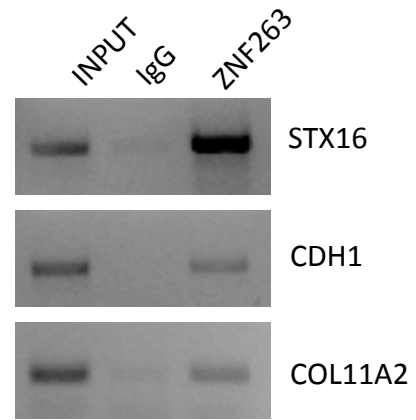
**Frieze\_Figure S1. Validation of the ZNF263 antibody.** (A) Nuclear extracts from the indicated cell types were analyzed by western blot using an antibody against ZNF263. (B) Nuclear extracts from K562 cells were subjected to immunoprecipitation using an antibody against ZNF263. The resultant immunoprecipitated fraction (IP) and supernatant (SN) were analyzed by western blot; also shown is a control immunoprecipitation using a nonspecific IgG antibody.



**Frietze\_Figure S2. (A) qPCR confirmation of ZNF263 ChIP-seq targets.** Binding sites identified by ChIP-seq were confirmed to be bound by ZNF263 in the two libraries (UCD27 and UCD64) that were used for sequencing; UCD27 and UCD64 are two independent libraries made from ZNF263 ChIP samples obtained using cultures of K562 cells grown on separate days. The relative enrichments of the target sites were determined by comparing qPCR signals from the ZNF263 libraries to the qPCR signals from an input library. **(B)** Eight ZNF263 targets identified by ChIP-seq were confirmed to be bound by ZNF263 in a third independent ChIP sample (not one of the ones used for the sequencing); three negative control regions (ZNF333, RAB37pro, and GAPDHpro) were also examined.



Frietze\_Supplementary Figure S3: To create a motif for searching genomic regions, each weblogo triplet (A), for the ZNF263 fingers (obtained using the program at <http://bioinfo.hanyang.ac.kr/ZIFIBI/frameset.php>) was turned into a nucleotide string, the nucleotide strings for the triplets were merged (B), and then the motif was written in the 5' to 3' direction (C); note: ZNFs bind in a C terminal to N terminal orientation, relative to the DNA sequence.



**Frietze\_Figure S4. ChIP-PCR analysis of the COL11A2 promoter.** Primers specific for a ZNF263 binding site identified using ChIP-seq (STX16), for a negative control (CDH1), and for the COL11A2 promoter were used to analyze a ZNF263 ChIP sample and a negative control IgG ChIP sample.



### ZNF263W1

$p = 1.24e-46$ , Core\_Score = 1.0, PWM\_Score = 1.0

**Frietze\_Supplementary Figure S5.** Secondary motif identified in the ZNF263 binding sites. A Weblog representing the 6 nt motif identified from 1297 ZNF263 binding sites lacking a primary ZNF263 motif. This motif resembles some of the AR binding motifs listed in the TRANSFAC database (see Supplementary Figure S6).

Frietze\_ Supplementary Figure S6. Transfac matrix similar to the secondary ZNF263 motif

```
AC M00962
XX
ID V$AR_Q6
XX
DT 18.11.2003 (created); dtc.
DT 18.11.2003 (updated); oke.
CO Copyright (C), Biobase GmbH.
XX
NA AR
XX
DE half-site matrix
XX
BF T00040; AR; Species: human, Homo sapiens.
BF T00041; AR; Species: mouse, Mus musculus.
BF T00042; AR; Species: rat, Rattus norvegicus.
BF T04652; AR; Species: baboon, Papio hamadryas.
BF T04653; AR; Species: Chimpanzee, Pan troglodytes.
BF T04654; AR; Species: macaque, Macaca fascicularis.
BF T04655; AR; Species: lemur, eulemur fulvus collaris.
XX
P0      A      C      G      T
01      11      2      4      13      W
02       1      5     23      1      G
03      26      0      1      3      A
04       8      1     20      1      G
05       4     22      1      3      C
06      29      1      0      0      A
07       8     12      5      5      N
08      11      0     13      6      R
09       9      6      6      9      N
XX
BA 30 compiled sequences
XX
BS tgagaacat; R03286; 9; 9;; n.
BS agaacaaaa; R10144; 7; 9;; n.
BS tgagtagat; R10148; -2; 9;; p.
BS tgaacaaga; R10149; 7; 9;; n.
BS agagcagga; R10150; 1; 9;; p.
BS agaacaatg; R10151; 7; 9;; n.
BS agagcatga; R10152; 1; 9;; p.
BS tgagaagaa; R14260; 3; 9;; p.
BS acagcaagt; R14261; 8; 9;; p.
BS tgagcaaag; R14262; 5; 9;; n.
BS tgtgcacac; R14263; 18; 9;; p.
BS taagcaagc; R14264; 23; 9;; p.
BS agatcatga; R14266; 32; 9;; n.
BS tttgcaagt; R14267; 23; 9;; n.
BS tgaccacag; R14276; 21; 9;; n.
BS aggacattc; R14281; 8; 9;; n.
BS ggagtactg; R14282; 7; 9;; n.
BS tgtacacgt; R14283; 16; 9;; p.
BS ccagcacac; R14284; 15; 9;; n.
BS ggagtactt; R14287; 12; 9;; p.
BS agaacaaga; R14293; 10; 9;; n.
BS agagccttt; R14294; 14; 9;; p.
BS tgagcacga; R14299; 10; 9;; n.
BS ggaacagaa; R14300; 13; 9;; n.
BS tgagaacag; R14301; 12; 9;; n.
BS agaacactg; R14302; 9; 9;; n.
BS ccagcaggc; R14306; 2; 9;; p.
BS tgagaacat; R14308; 11; 9;; n.
BS gcagcacgc; R14312; 5; 9;; p.
BS acaggatgt; R14314; 4; 9;; p.
XX
CC half-site of ARE (androgen response element)
XX
RN [1]; RE0017571.
RA TRANSFAC Team.
RT New TRANSFAC MATRIX entries
RL TRANSFAC Reports 3:0001 (2002).
XX
```

| A            |                         |
|--------------|-------------------------|
| ID           | V\$ZNF263K562M11        |
| MATR_LENGTH  | 24                      |
| CORE_START   | 18                      |
| CORE_LENGTH  | 5                       |
| CORE_MAXIMAL | 5968                    |
| MAXIMAL      | 23969                   |
| FREQ_T       | 0.0506504585199403      |
| FREQ_A       | 0.330534229046705       |
| FREQ_C       | 0.0622734058434634      |
| FREQ_G       | 0.556541906589891       |
| 1            | A:384 C:65 G:1042 T:72  |
| 2            | A:703 C:50 G:783 T:27   |
| 3            | A:478 C:39 G:962 T:84   |
| 4            | A:390 C:148 G:999 T:26  |
| 5            | A:1009 C:42 G:305 T:207 |
| 6            | A:200 C:61 G:1263 T:39  |
| 7            | A:298 C:119 G:1103 T:43 |
| 8            | A:888 C:79 G:520 T:76   |
| 9            | A:459 C:101 G:931 T:72  |
| 10           | A:319 C:145 G:958 T:141 |
| 11           | A:669 C:161 G:659 T:74  |
| 12           | A:406 C:206 G:886 T:65  |
| 13           | A:447 C:181 G:830 T:105 |
| 14           | A:693 C:115 G:643 T:112 |
| 15           | A:331 C:67 G:909 T:256  |
| 16           | A:245 C:172 G:1097 T:49 |
| 17           | A:934 C:30 G:496 T:103  |
| 18           | A:247 C:27 G:1267 T:22  |
| 19           | A:357 C:177 G:1024 T:5  |
| 20           | A:1142 C:57 G:184 T:180 |
| 21           | A:267 C:16 G:1224 T:56  |
| 22           | A:133 C:104 G:1311 T:15 |
| 23           | A:1024 C:22 G:460 T:57  |
| 24           | A:376 C:152 G:1021 T:14 |

| B            |                         |
|--------------|-------------------------|
| ID           | ZNF263_Predicted_Half_L |
| MATR_LENGTH  | 12                      |
| CORE_START   | 4                       |
| CORE_LENGTH  | 5                       |
| CORE_MAXIMAL | 3153                    |
| MAXIMAL      | 6941                    |
| FREQ_T       | 0.0142276422764228      |
| FREQ_A       | 0.343241869918699       |
| FREQ_C       | 0.0107977642276423      |
| FREQ_G       | 0.631732723577236       |
| 1            | A:212 C:42 G:365 T:37   |
| 2            | A:261 C:16 G:347 T:32   |
| 3            | A:0 C:0 G:656 T:0       |
| 4            | A:0 C:0 G:656 T:0       |
| 5            | A:656 C:0 G:0 T:0       |
| 6            | A:102 C:6 G:529 T:19    |
| 7            | A:0 C:0 G:656 T:0       |
| 8            | A:656 C:0 G:0 T:0       |
| 9            | A:159 C:21 G:452 T:24   |
| 10           | A:0 C:0 G:656 T:0       |
| 11           | A:0 C:0 G:656 T:0       |
| 12           | A:656 C:0 G:0 T:0       |

| C            |                         |
|--------------|-------------------------|
| ID           | ZNF263_Predicted_Half_R |
| MATR_LENGTH  | 12                      |
| CORE_START   | 2                       |
| CORE_LENGTH  | 5                       |
| CORE_MAXIMAL | 2362                    |
| MAXIMAL      | 5292                    |
| FREQ_T       | 0.0144781144781145      |
| FREQ_A       | 0.329124579124579       |
| FREQ_C       | 0.0164983164983165      |
| FREQ_G       | 0.6398989898989899      |
| 1            | A:218 C:24 G:212 T:41   |
| 2            | A:0 C:0 G:495 T:0       |
| 3            | A:0 C:0 G:495 T:0       |
| 4            | A:0 C:0 G:495 T:0       |
| 5            | A:495 C:0 G:0 T:0       |
| 6            | A:79 C:17 G:382 T:17    |
| 7            | A:57 C:34 G:399 T:5     |
| 8            | A:495 C:0 G:0 T:0       |
| 9            | A:116 C:23 G:333 T:23   |
| 10           | A:0 C:0 G:495 T:0       |
| 11           | A:0 C:0 G:495 T:0       |
| 12           | A:495 C:0 G:0 T:0       |

| D   |     |   |   |   |     |   |   |     |    |    |    |     |    |    |    |    |    |    |    |     |    |    |    |
|-----|-----|---|---|---|-----|---|---|-----|----|----|----|-----|----|----|----|----|----|----|----|-----|----|----|----|
| 1   | 2   | 3 | 4 | 5 | 6   | 7 | 8 | 9   | 10 | 11 | 12 | 13  | 14 | 15 | 16 | 17 | 18 | 19 | 20 | 21  | 22 | 23 | 24 |
| N   | N   | G | G | A | N   | G | A | N   | G  | G  | A  | N   | G  | G  | A  | N  | N  | A  | N  | G   | G  | A  |    |
| G/A | G/A | G | G | A | G/A | G | A | G/A | G  | G  | A  | A/G | G  | G  | G  | A  | G  | G  | A  | G/A | G  | G  | A  |

**Frietze\_Supplementary Figure S7.** PWMs of the binding site matches to the experimentally derived and predicted ZNF263 motifs. Shown in panel A is the nucleotide distribution at each of the 24 positions for the de novo ZNF263 motif derived from the ChIP-seq data (see Figure 4A). For panel B and C, the sequences that matched the left (panel B) or right (panel C) half of the predicted motif (see Figure 4B) and that fell within 200 bp of either side of the center of a ZNF263 ChIP-seq peak were identified. Shown are the nucleotide distributions for the PWM derived from these matches to each half of the predicted motif. Shown in panel D is a comparison of the newly derived motifs from panel B and C (bottom line) to the predicted motif (top line); shown in yellow are the positions not specified by the zinc finger code but highly specified in the binding sites.